Radiology

ORIGINAL RESEARCH • NEURORADIOLOGY

Maximum Resection of Noncontrast-enhanced Tumor at MRI Is a Favorable Prognostic Factor in IDH Wild-Type Glioblastoma

Hye Hyeon Moon, MD, PhD[*1] • *Doonyaporn Wongsawaeng, MD*[*6] • *Ji Eun Park, MD, PhD*[1] • *Seo Young Park, PhD*[9] • *Seunghee Baek, PhD*[3] • *Young-Hoon Kim, MD, PhD*[4] • *Sang Woo Song, MD, PhD*[4] • *Chang-Ki Hong, MD, PhD*[4] • *Jeong Hoon Kim, MD, PhD*[4] • *Myung Hwan Lee, MD, PhD*[5] • *Yae Won Park, MD, PhD*[5] • *Sung Soo Ahn, MD, PhD*[5] • *Jeffrey Michael Pollock, MD*[2] • *Ramon Francisco Barajas Jr, MD*[2,7,8] • *Ho Sung Kim, MD, PhD*[1]

* H.H.M. and D.W. contributed equally to this work.

Author affiliations, funding, and conflicts of interest are listed at the end of this article.

Radiology 2025; 315(2):e241393 • https://doi.org/10.1148/radiol.241393 • Content codes: NR MR

Background: Isocitrate dehydrogenase (IDH) wild-type glioblastoma often includes a noncontrast-enhanced tumor (NET) component, and the extent of NET resection may serve as a prognostic marker.

Purpose: To assess clinical outcomes based on gross total resection (GTR) of NET, develop a real-world survival model incorporating GTR-NET for IDH wild-type glioblastoma, and validate the findings in multinational external cohorts.

Materials and Methods: A retrospective analysis included patients with IDH wild-type glioblastoma in a prospective registry (March 2017 to October 2020) as the training set. External validation used consecutive patients from two centers (March 2017 to January 2023). Patients were stratified into three groups: GTR-NET, GTR in contrast-enhanced tumor (CET) only, and no GTR. A conditional inference tree (CIT) model was developed using GTR type, age, and O^6-methylguanine DNA methyltransferase (*MGMT*) promoter methylation status to predict overall survival (OS) and was externally validated. Kaplan-Meier analysis, log-rank test, time-dependent area under the receiver operating characteristic curve, and Harrell C-indexes were used for evaluation.

Results: In the training set (n = 201; mean age, 60 years ± 11.3; 109 males), four survival groups were identified. GTR-NET was associated with longer OS (median, 32.6 months; IQR, 18.7–46.7 months; P < .001). When GTR-NET was not achieved, OS was stratified as follows: younger than age 60 years (median OS, 23.4 months; IQR, 12.2–34.8 months), age 60 years or older and positive for *MGMT* (median OS, 19.1 months; IQR, 13.0–27.8 months), and age 60 years or older and negative for *MGMT* (median OS, 10.7 months; IQR, 6.5–14.1 months). External validation sets (352 patients in external validation set 1 and 60 patients external validation set 2) confirmed these groups (P < .001 and P = .04). Time-dependent areas under the receiver operating characteristic curve ranged from 0.684 (95% CI: 0.623, 0.745) to 0.694 (95% CI: 0.631, 0.758) and from 0.610 (95% CI: 0.449, 0.771) to 0.678 (95% CI: 0.512, 0.844), with CIT sensitivity for GTR-NET at 70.7%–77.3% and 87.6%–87.9% and C-indexes of 0.65 and 0.63.

Conclusion: A GTR-NET–based survival model was developed and validated, demonstrating that GTR-NET is an independent prognostic marker for longer OS in IDH-wildtype glioblastoma.

ClinicalTrials.gov identifier: NCT02619890

Supplemental material is available for this article.

In the World Health Organization, or WHO, 2021 classification, isocitrate dehydrogenase (IDH)–wild-type glioblastoma is designated as a distinct diagnosis on the basis of IDH genetic testing (1). This classification encompasses not only typical contrast-enhanced necrotic tumors but also ill-defined infiltrative tumors that are not enhanced. Maximal safe resection is a goal of surgery for glioblastoma (2–4), and gross total resection (GTR) of contrast-enhanced tumor (CET) is associated with longer survival (2,5–7). Historically, emphasis has been predominantly placed on the extent of resection (EOR) of the CET, whereas the noncontrast-enhanced tumor (NET) has received relatively less attention. Given that IDH–wild-type glioblastoma (per the WHO 2021 Classification of Tumors of the Central Nervous System [1]) frequently contains a NET portion, the concept of "supramaximal" resection beyond CET borders has emerged, and survival benefits have been observed in retrospective studies (8).

Recently, the Response Assessment in Neuro-Oncology (RANO) resection group proposed a new classification system for EOR in glioblastoma that considers both CET and NET, and validated the value of this system for predicting overall survival (OS) (9). Extensive resection of NET (≤5 cm^3 residual NET) has been shown to provide additional survival benefits, justifying the introduction of a new EOR category, supramaximal resection. This EOR represents a shift away from focusing solely on CET for survival stratification. For prognostic modeling of IDH wild-type glioblastoma, it is essential to consider prognostically important variables, including age, performance status (10), and O^6-methylguanine DNA methyltransferase (*MGMT*) promoter methylation status (11,12), whenever EOR analysis is undertaken. Although supramaximal resection has become an important prognostic factor for IDH wild-type glioblastomas, an integrative survival model incorporating clinical and molecular profiles is lacking. Additionally, the real-world feasibility of this EOR needs to be tested in multicenter and multinational analyses. A simple and clinically applicable prognostic classification system based on EOR for CET and NET, key molecular

Abbreviations

CET = contrast-enhanced tumor, CIT = conditional inference tree, EOR = extent of resection, FLAIR = fluid-attenuated inversion recovery, GTR = gross total resection, HR = hazard ratio, IDH = isocitrate dehydrogenase, *MGMT* = O^6-methylguanine DNA methyltransferase, NET = noncontrast-enhanced tumor, OS = overall survival, RANO = Response Assessment in Neuro-Oncology

Summary

Gross total resection of noncontrast-enhanced tumor was an independent prognostic factor for longer overall survival, regardless of age and O^6-methylguanine DNA methyltransferase promoter methylation status, in patients with isocitrate dehydrogenase wild-type glioblastoma.

Key Results

- In a retrospective study of prospective registry data from 201 patients with isocitrate dehydrogenase wild-type glioblastoma, gross total resection (GTR) of noncontrast-enhanced tumor (NET) on MRI scans was associated with longer overall survival (log-rank $P < .001$).
- Conditional inference trees to stratify patients according to GTR-NET, age, and O^6-methylguanine DNA methyltransferase promoter methylation status were validated in two external validation sets, and GTR-NET time-dependent sensitivity was consistent up to 2 years in both sets (70.7%–77.3% and 87.6%–87.9%).

markers, and clinical variables would aid patient consultation and treatment planning.

Thus, the purpose of this study was to assess clinical outcomes based on GTR of NET, develop a real-world survival model incorporating GTR-NET for IDH wild-type glioblastoma, and validate the findings in multinational external cohorts

Materials and Methods

Study Patients

This study was approved by the institutional review board of Asan Medical Center (Seoul, Korea; institutional review board number 2022–0459). This study was a retrospective analysis of prospectively collected data in a brain tumor registry (ClinicalTrials.gov registry number NCT02619890), and informed consent was obtained from all patients. The Strengthening the Reporting of Observational Studies in Epidemiology, or STROBE, reporting guidelines were followed for this study. The inclusion criteria were as follows: newly diagnosed IDH wild-type glioblastoma, per the WHO 2021 Classification of Tumors of the Central Nervous System, with histopathologic confirmation and known *MGMT* promoter methylation status; treatment with standard concurrent chemotherapy and radiation therapy and temozolomide according to the Stupp regimen; and age older than 18 years. Patients were excluded if they had a history of surgery; they did not undergo follow-up imaging until 6 months after the completion of standard treatment according to the Stupp regimen (13); their postoperative imaging data (including diffusion-weighted imaging data) were missing; or they had H3 K27M alterations and were therefore diagnosed with diffuse midline glioma, H3 K27–altered. Consecutive patients included in the registry who underwent standard concurrent chemoradiation therapy between March 2017 and October 2020 were evaluated for eligibility for inclusion in the training set.

Consecutive patients from Severance Hospital (Seoul, Korea) between March 2017 and October 2020 and from Oregon Health and Science University Hospital (Portland, Ore) between March 2018 and January 2023 meeting these same criteria were included in external validation sets 1 and 2, respectively.

The following covariables were obtained for each patient through medical chart review: age, sex, Karnofsky performance status score at diagnosis, *MGMT* promoter methylation status, epidermal growth factor receptor expression status, and telomerase reverse transcriptase promoter mutation status. Details of the molecular classification can be found in Appendix S1. Tumor size and location were assessed at preoperative MRI. Tumor size was measured by the two-dimensional diameter method (the sum of the products of the perpendicular diameters of contrast-enhanced lesions on contrast-enhanced T1-weighted images), as recommended by RANO (14). Tumor location was classified into frontal, temporal, deep, multifocal, or other categories. OS was calculated from the date of diagnosis to the date of death from any cause, ascertained by national health care system linkage. Patients were censored at the date of medical record abstraction or the date of the last imaging report, whichever came first.

MRI Protocols

Preoperative and postoperative MRI (performed within 72 hours after operation), including T1-weighted, T2-weighted, fluid-attenuated inversion recovery (FLAIR), three-dimensional contrast-enhanced T1-weighted, and diffusion-weighted imaging, were performed. Details of the MRI protocols used in the training set and two external validation sets are provided in Table S1.

Definition of the EOR Types

The definitions of the EOR types are presented in Figure 1. There were three EOR types: GTR of NET (GTR-NET), GTR of CET but not NET (GTR-CET), and no GTR. GTR-CET was defined as no evidence of remnant measurable or nonmeasurable contrast-enhanced lesions at postoperative MRI. GTR-NET was defined as no evidence of a remnant infiltrative T2-weighted or FLAIR hyperintense or intermediate lesion at postoperative MRI. Because distinguishing NET from peritumoral edema is crucial, a detailed explanation is provided in Table S2. NET is defined as relatively mild FLAIR hyperintensity, gray matter involvement, eccentric extension beyond anatomic constraints, focal parenchymal expansion, and mass effect (15–18). However, edema is typically confined to white matter, sparing the cortical ribbon and deep gray matter, and usually manifests as marked FLAIR hyperintensity (19). The reviewers confirmed that the postoperative T2-weighted or FLAIR hyperintensities were not the result of surgically induced edema or ischemia. Details regarding interreader agreement and quantitative analysis of the EOR types are available in Appendix S1 and Table S3.

Statistical Analysis

Details of the descriptive and comparative statistics are in Appendix S1. Univariable and multivariable Cox analyses were performed to determine predictors of OS using EOR of CET and NET, with clinical and molecular factors (age, sex, Karnofsky performance status score, tumor size, tumor location, *MGMT* promoter methylation, epidermal growth factor

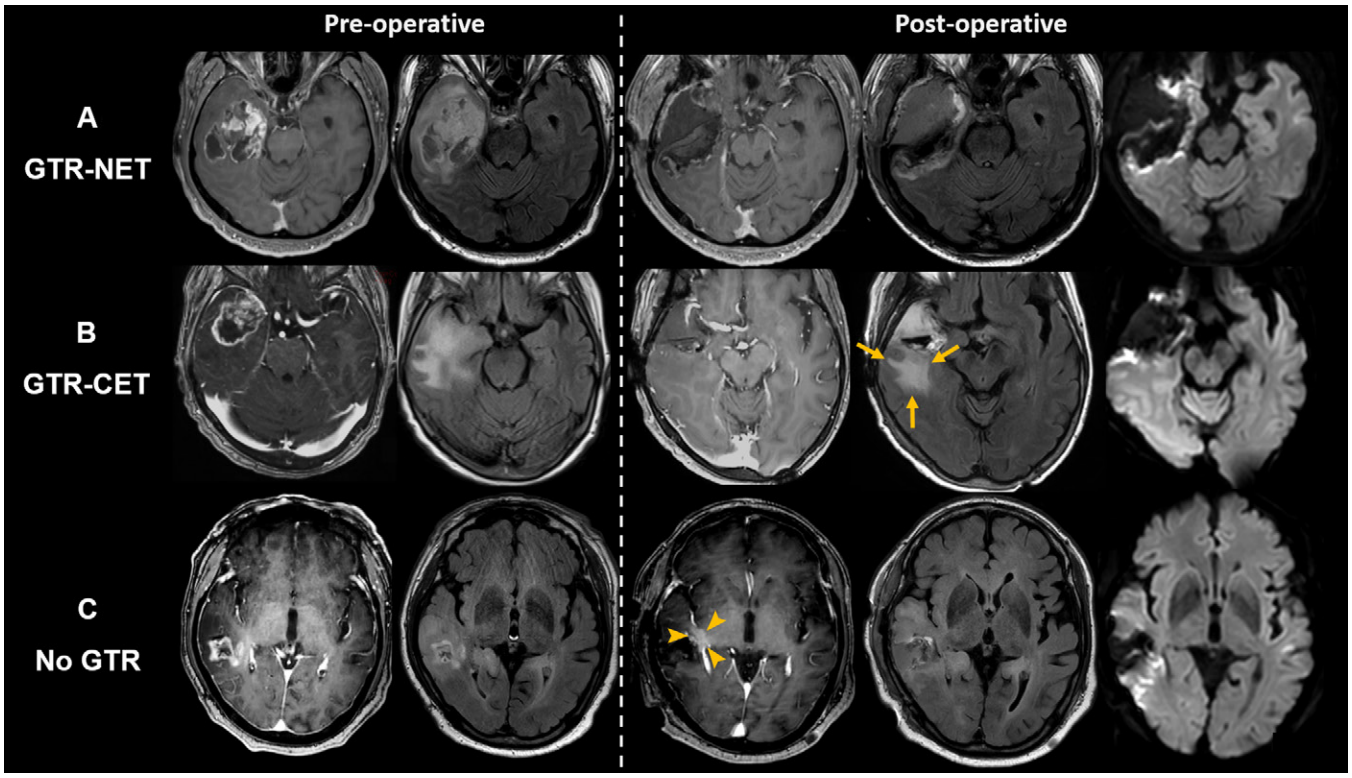

Figure 1: Axial MRI scans show extent-of-resection groups for **(A)** gross total resection (GTR) of both contrast-enhanced tumor (CET) and noncontrast-enhanced tumor (NET) (GTR-NET), **(B)** GTR of CET but NET remained (GTR-CET), and **(C)** no GTR. Scans show **(B)** residual T2 and fluid-attenuated inversion recovery (FLAIR) high-signal infiltrative tumor (arrows) and **(C)** residual CET around the surgical cavity (arrowheads). Diffusion-weighted imaging (right-side column) was used to differentiate residual T2-weighted or FLAIR signal hyperintensity as a result of NET from cytotoxic surgery-induced changes.

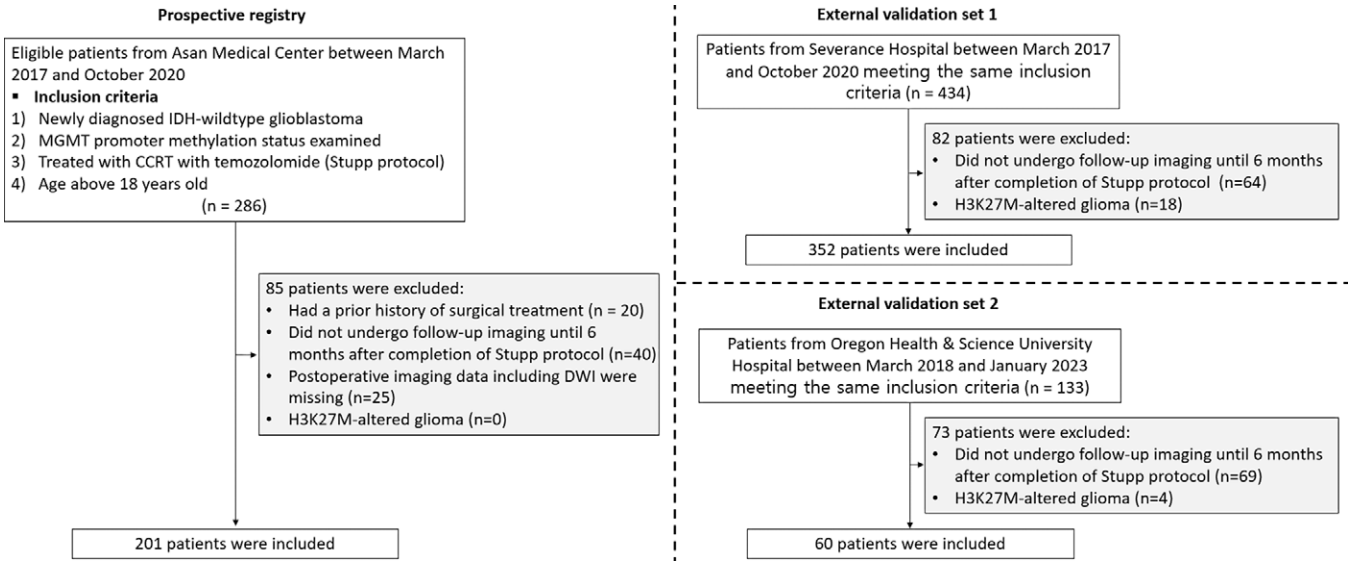

Figure 2: Flow diagram of patient recruitment for the training set and external validation sets 1 and 2. CCRT = concurrent chemoradiation therapy, DWI = diffusion-weighted imaging, IDH = isocitrate dehydrogenase, *MGMT* = O^6-methyguanine-DNA methyltransferase.

receptor amplification, and telomerase reverse transcriptase promoter mutation). Further details of this method are available in Appendix S1.

The survival model was developed by conditional inference tree (CIT) analysis (ie, classification and regression tree analysis), in which recursive partitioning and permutation testing were used to reduce overfitting and bias (20). CIT analysis creates a series of binary splits (nodes) from demographic, molecular, and clinical variables (age, sex, Karnofsky performance status score, tumor size, tumor location, EOR of CET, EOR of NET, *MGMT* promoter methylation status, epidermal growth factor receptor amplification, and telomerase reverse transcriptase promoter mutation status) to generate decision rules for predicting OS. Further details of this method are available in Appendix S1.

Table 1: Baseline Clinical Characteristics of the Study Patients

Parameter	Training Set (*n* = 201)	External Validation Set 1(*n* = 352)		External Validation Set 2 (*n* = 60)	
		Set 1	*P* Value	Set 2	*P* Value
Sex			.15		.43
Male	109 (54.2)	213 (60.5)		36 (60)	
Female	92 (45.8)	139 (39.5)		24 (40)	
Age at diagnosis (y)*	60.0 ± 11.3	61.4 ± 12.0	.18	63.0 ± 9.9	.23
KPS score at diagnosis			<.001		<.001
NA	0 (0)	0 (0)		14 (23.3)	
<60	0 (0)	20 (5.7)		1 (1.7)	
60	14 (7.0)	20 (5.7)		0 (0)	
70	15 (7.5)	33 (9.4)		9 (15)	
80	61 (30.3)	79 (22.4)		11 (18.3)	
90	60 (29.9)	174 (49.4)		18 (30)	
100	51 (25.4)	26 (7.4)		7 (11.7)	
Tumor size (cm^2)*	18 ± 9.82	16.2 ± 10.7	.01	13.5 ± 10.5	.001
Tumor location			.02		.02
Frontal or temporal lobe	128 (63.7)	194 (55.1)		39 (65)	
Others	51 (25.4)	83 (23.6)		10 (16.7)	
Deep	13 (6.5)	41 (11.6)		2 (3.3)	
Multifocal	9 (4.5)	34 (9.7)		9 (15)	
EOR of CET			.02		.002
GTR	124 (61.7)	251 (71.3)		24 (40)	
Others†	77 (38.3)	101 (28.7)		36 (60)	
EOR of NET			.21		.009
GTR	72 (35.8)	145 (41.2)		10 (16.7)	
Others‡	129 (64.2)	207 (58.8)		50 (83.3)	
MGMT promoter methylation			>.99		.98
Methylated	80 (39.8)	140 (39.8)		24 (40)	
Unmethylated	121 (60.2)	212 (60.2)		36 (60)	
EGFR amplification			<.001		<.001
Amplified	59 (29.4)	114 (32.4)		33 (55)	
Not amplified	116 (57.7)	235 (66.8)		12 (20)	
NA	26 (12.9)	3 (0.9)		15 (25)	
TERTp mutation status			<.001		<.001
Mutated	57 (28.4)	211 (59.9)		34 (56.7)	
Wild-type	113 (56.2)	140 (39.8)		11 (18.6)	
NA	31 (15.4)	1 (0.3)		15 (25)	
Median follow-up (mo)‡	15.6 (8–26.4)	21.7 (13.7–29.6)	.005	12.0 (6.5–24.9)	.26

Note.—Unless otherwise indicated, data are numbers of patients, and data in parentheses are percentages. *P* values indicate comparison between training and external validation sets. Differences in categorical variables between the training and validation sets were assessed by using the Fisher exact test and the χ^2 test, and differences between continuous variables were assessed by using the Student *t* test or Mann-Whitney *U* test according to the results of normality testing. CET = contrast-enhanced tumor, *EGFR* = epidermal growth factor receptor, EOR = extent of resection, GTR = gross total resection, KPS = Karnofsky performance status, *MGMT* = O^6-methylguanine-DNA methyltransferase, NA = not applicable, NET = noncontrast-enhanced tumor, *TERTp* = telomerase reverse transcriptase promoter.

* Data are means ± SDs.

† Subtotal resection, partial resection, and biopsy.

‡ Data in parentheses are IQRs.

The Kaplan-Meier method was used to draw OS curves for each node derived from the CIT, and the log-rank test was used to compare the curves. The prognostic performance of the CIT-based survival model was evaluated via the Harrell *C* index and time-dependent receiver operating characteristic curve analysis (21), which was used to calculate the 1- and 2-year areas under the receiver operating characteristic curve. C-index values of less than 0.6, 0.6–0.7, and greater than 0.7 for the prognostic models were considered poor, moderate, and good, respectively (22). Binary discrimination performance was also calculated by time-dependent sensitivity and specificity for each year, comparing CIT group 1 (lower risk) with CIT groups 2, 3, and 4 (higher risk).

An established rule of thumb of ensuring at least 10 events for each predictor parameter to calculate the sample size was used (23). Based on this guideline, our training set of 201 patients with 101 events provided sufficient power for survival model derivation.

Table 2: Univariable and Multivariable Cox Proportional Hazards Regression Analyses to Determine Predictors of Overall Survival in Patients with IDH Wild-Type Glioblastoma in the Training Set

	Univariable Analysis			Multivariable Analysis		
Parameter	Regression Coefficient	HR	*P* Value	Regression Coefficient	HR	*P* Value
Age	0.02	1.02 (1.00, 1.04)	.03	0.03	1.03 (1.01, 1.05)	.004
Sex (male as reference)	−0.40	0.67 (0.45, 0.99)	.13			
KPS score	−0.02	0.98 (0.97, 0.99)	.05	−0.02	0.98 (0.96, 1.00)	.12
Tumor size	0	1.00 (0.98, 1.03)	.89			
Tumor location			.04			.16
Frontal or temporal lobe	Ref			Ref		
Others	−0.56	0.57 (0.31, 1.04)	.07	−0.34	0.71 (0.42, 1.19)	.20
Deep	−0.12	0.89 (0.36, 2.23)	.80	0.15	1.16 (0.52, 2.58)	.72
Multifocal	0.80	2.23 (1.03, 5.05)	.04	0.73	2.08 (0.90, 4.80)	.09
MGMT promotor status (unmethylated as reference)	−0.42	0.66 (0.44, 0.98)	.04	−0.82	0.44 (0.29, 0.68)	.001
EGFR amplification (not amplified as reference)	0.08	1.08 (0.67, 1.74)	.75			
TERTp mutation status (wild-type as reference)	−0.12	0.89 (0.50, 1.55)	.66			
EOR*						
GTR-CET	−0.76	0.48 (0.33, 0.72)	<.001	−0.06	0.94 (0.55, 1.58)	.81
GTR-NET	−1.02	0.36 (0.23, 0.57)	<.001	−1.20	0.30 (0.19, 0.47)	<.001

Note.—Univariable and multivariable Cox proportional hazards regression analyses were performed to determine predictors of overall survival in patients with IDH wild-type glioblastoma in the training set. *P* values were calculated using the Wald test for all variables listed in the table. Variables with $P < .10$ at univariable analysis were included in the multivariable analysis by forward stepwise selection on the basis of the Akaike information criterion. CET = contrast-enhanced tumor, *EGFR* = epidermal growth factor receptor, EOR = extent of resection, GTR = gross total resection, HR = hazard ratio, KPS = Karnofsky performance status, *MGMT* = O⁶-methylguanine-DNA methyltransferase, NET = noncontrast-enhanced tumor, Ref = reference, *TERTp* = telomerase reverse transcriptase promoter.

* HRs for GTR were calculated by referencing the non-GTR for comparison with other variables.

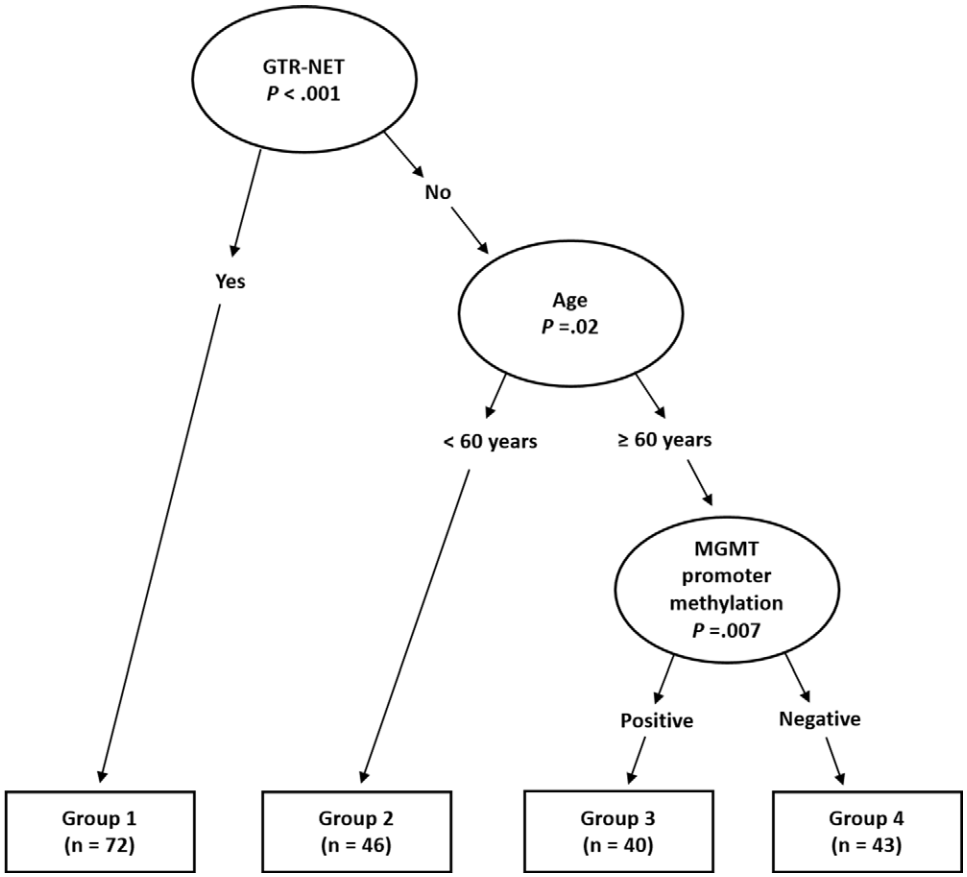

Figure 3: A survival model plot uses the training dataset for conditional inference tree regression and shows that gross total resection (GTR) of noncontrast-enhanced tumor (NET) was the best predictor of overall survival (OS) in patients with isocitrate-dehydrogenase wild-type glioblastoma. To use the model, a clinician first follows the tree path provided by assessing each variable for a patient and then follows the path to the final node that gives the predicted OS. Group 1 is GTR-NET, group 2 is no GTR-NET and age younger than 60 years, group 3 is no GTR-NET and age older than 60 years and positive O⁶-methyguanine-DNA methyltransferase (*MGMT*) status, and group 4 is no GTR-NET and age older than 60 years and negative *MGMT* status. Negative indicates negative status, positive indicates positive status.

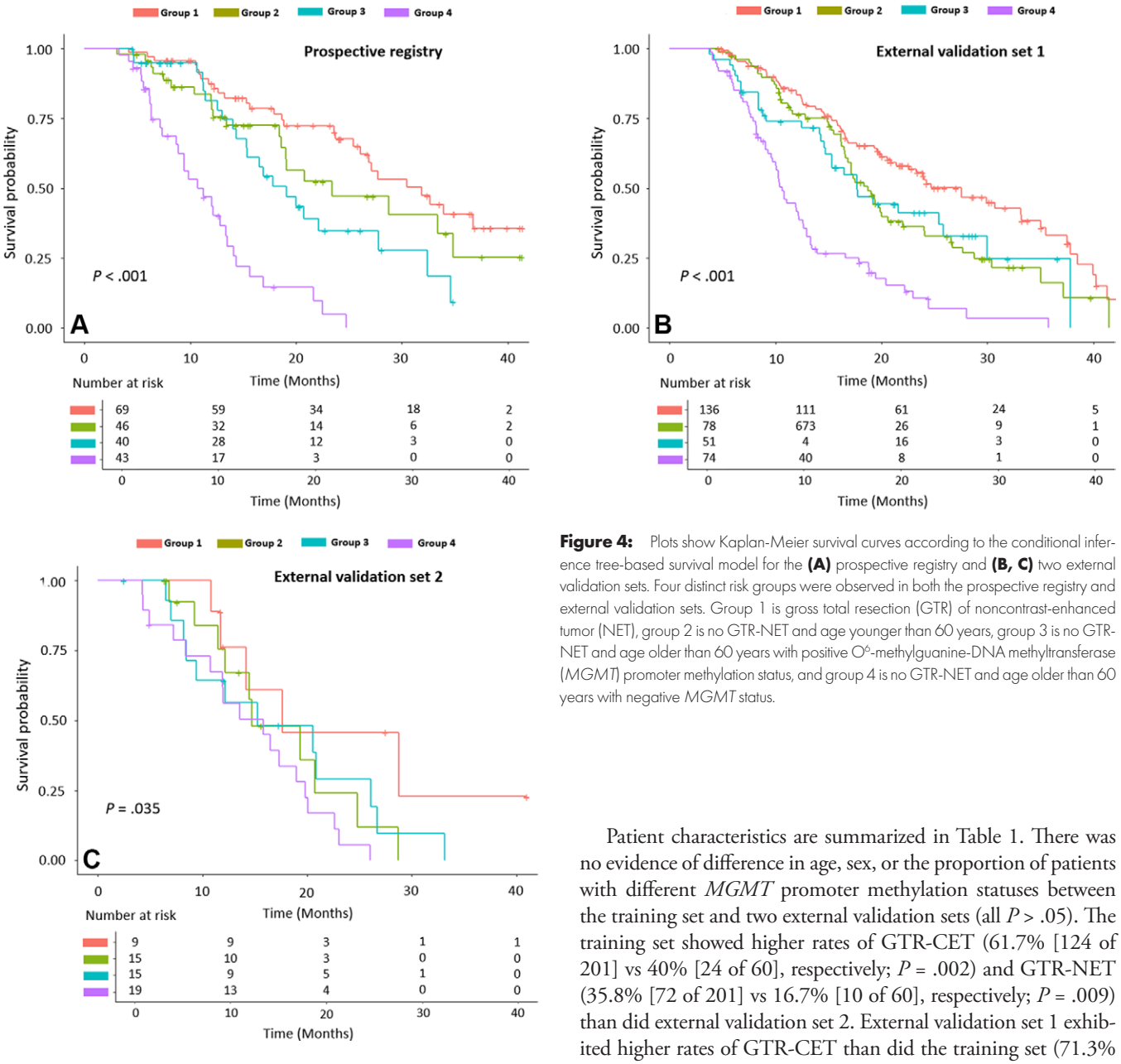

Figure 4: Plots show Kaplan-Meier survival curves according to the conditional inference tree-based survival model for the **(A)** prospective registry and **(B, C)** two external validation sets. Four distinct risk groups were observed in both the prospective registry and external validation sets. Group 1 is gross total resection (GTR) of noncontrast-enhanced tumor (NET), group 2 is no GTR-NET and age younger than 60 years, group 3 is no GTR-NET and age older than 60 years with positive O^6-methylguanine-DNA methyltransferase (*MGMT*) promoter methylation status, and group 4 is no GTR-NET and age older than 60 years with negative *MGMT* status.

Statistical analyses were performed by using software (R, version 4.0.2; R Foundation for Statistical Computing, R Core Team) by expert statisticians (S.B. and S.Y.P., both with 15 years of experience in biostatistics), using the packages partykit and ctree. Two-sided $P < .05$ was indicative of statistical significance.

Results

Patient Characteristics

The patient flowchart is presented in Figure 2. Details regarding patient inclusion and exclusion are provided in Appendix S1. This study included 201 patients in the training set, 352 patients in external validation set 1, and 60 patients in external validation set 2. The median follow-up periods in the training set, external validation set 1, and external validation set 2 were 15.6 months (IQR, 8–26.4 months), 21.7 months (IQR, 13.7–29.6 months), and 12.0 months (IQR, 6.5–24.9 months), respectively.

Patient characteristics are summarized in Table 1. There was no evidence of difference in age, sex, or the proportion of patients with different *MGMT* promoter methylation statuses between the training set and two external validation sets (all $P > .05$). The training set showed higher rates of GTR-CET (61.7% [124 of 201] vs 40% [24 of 60], respectively; $P = .002$) and GTR-NET (35.8% [72 of 201] vs 16.7% [10 of 60], respectively; $P = .009$) than did external validation set 2. External validation set 1 exhibited higher rates of GTR-CET than did the training set (71.3% [251 of 352] vs 61.7% [124 of 201], respectively; $P = .02$). Karnofsky performance status scores, tumor size, tumor location, epidermal growth factor receptor amplification, and telomerase reverse transcriptase promoter mutation status were different between the training set and two external validation sets (all $P < .05$), reflecting their clinical and molecular heterogeneity.

Univariable and Multivariable Cox Analyses to Determine Predictors of OS

In the training set, univariable Cox analysis showed that age (hazard ratio [HR], 1.02; 95% CI: 1.00, 1.04; $P = .03$), tumor location ($P = .04$), *MGMT* promoter methylation status (HR, 0.66; 95% CI: 0.44, 0.98; $P = .04$), GTR-CET (HR, 0.48; 95% CI: 0.33, 0.72; $P < .001$), and GTR-NET (HR, 0.36; 95% CI: 0.23, 0.57; $P < .001$) were associated with OS. At multivariable Cox analysis, age (HR, 1.03; 95% CI: 1.01, 1.05; $P = .004$), *MGMT* promoter methylation status (HR, 0.44; 95% CI: 0.29, 0.68; $P = .001$), and GTR-NET (HR, 0.30; 95% CI: 0.19, 0.47; $P < .001$) were independent prognostic factors (Table 2).

Table 3: Time-dependent Discrimination Measures for Deaths Up to 2 Years in the Training and External Validation Sets

	Time-dependent AUC			Time-dependent Sensitivity (%)			Time-dependent Specificity (%)		
Parameter	Training Set	External Set 1	External Set 2	Training Set	External Set 1	External Set 2	Training Set	External Set 1	External Set 2
1 y	0.704 (0.610, 0.798)	0.694 (0.631, 0.758)	0.610 (0.449, 0.771)	79.8 (67.3, 92.3)	77.3 (68.7, 85.8)	87.9 (72.0, 100)	45.2 (36.4, 53.9)	47.4 (40.9, 53.9)	18.2 (4.9, 31.5)
2 y	0.770 (0.693, 0.846)	0.684 (0.623, 0.745)	0.678 (0.512, 0.844)	77.7 (68.5, 86.9)	70.7 (63.9, 77.4)	87.6 (76.2, 99.1)	64.6 (51.0, 78.1)	55.7 (45.3, 66.1)	30.8 (5.5, 56.1)

Note.—Data in parentheses are 95% CIs. The sensitivity and specificity are referenced for conditional inference tree group 1 (gross tumor resection of noncontrast-enhanced tumor [NET]) versus groups 2, 3, and 4 (no gross tumor resection of NET). AUC = area under the receiver operating characteristic curve.

OS Stratified by CIT Analysis

For the CIT analysis, patients were divided into four groups. Figure 3 shows the survival model constructed with the CIT. The first group consisted of patients who underwent GTR-NET ($P < .001$) and was composed of 72 patients with a median OS of 32.6 months (IQR, 18.7–46.7 months). Among patients in whom GTR-NET was not achieved, the second group ($n = 46$) consisted of those aged younger than 60 years, with a median OS of 23.4 months (IQR, 12.2–34.8 months; $P = .02$). The third group ($n = 40$) consisted of patients aged 60 years or older who were positive for *MGMT* promoter methylation and in whom GTR-NET was not achieved, with an OS of 19.1 months (IQR, 13.0–27.8 months; $P = .007$). Finally, the fourth group ($n = 43$) consisted of patients aged 60 years or older with an unmethylated *MGMT* promoter status in whom GTR-NET was not achieved, with the shortest OS of 10.7 months (IQR, 6.5–14.1 months; $P = .007$).

In the training set, univariable Cox regression analyses were conducted for the CIT groups, along with clinical and molecular factors, with the first group used as the reference (Table S4). The fourth group had shorter OS than did the first group (HR, 7.34; 95% CI: 3.91, 13.8; $P < .001$), followed by the third group (HR, 1.94; 95% CI: 1.02, 3.67; $P = .04$).

Similarly, in external validation set 1, univariable analysis also showed an association between CIT groups and OS (Table S4). Compared with the first group, the fourth group had shorter OS (HR, 4.04; 95% CI: 2.84, 5.74; $P < .001$), followed by the third group (HR, 1.81; 95% CI: 1.17, 2.79; $P = .007$) and the second group (HR, 1.65; 95% CI: 1.16, 2.36; $P = .006$). In external validation set 2, the fourth group also had shorter OS than the first group (HR, 6.32; 95% CI: 1.28, 31.3; $P = .02$).

Prognostic Performance of the Survival Model in the External Validation Set

The survival model based on the CIT analysis was applied to two external validation sets. Figure 4 shows the Kaplan-Meier survival curves for each risk group derived from the CIT analysis in both the training and external validation sets, successfully stratifying the prognosis. In external validation set 1, the median OS times for the first, second, third, and fourth groups were 30.4 months (95% CI: 23.7, 38.1), 19.4 months (95% CI: 17.1, 24.4), 18.0 months (95% CI: 14.8, 38.5), and 10.8 months (95% CI: 9.8, 12.8) ($P < .001$), respectively. In external validation set 2, the median OS times for the first, second, third, and fourth groups were 28.8 months (95% CI: 10.8, 28.7), 19.3 months (95% CI: 11.5, 68.4), 15.2 months (95% CI: 8.2, 33.11), and 13.5 months (95% CI: 8.4, 26.0) ($P = .04$), respectively.

The prognostic performance of the CIT-based model is in Table 3 and Figure S1. The C-index for the CIT-based model was 0.69 (95% CI: 0.63, 0.74) in the training set, 0.65 (95% CI: 0.61, 0.68) in external validation set 1, and 0.63 (95% CI: 0.54, 0.72) in external validation set 2, indicating moderate performance. The time-dependent area under the receiver operating characteristic curve values for 1 year and 2 years were 0.694 (95% CI: 0.631, 0.758) and 0.684 (95% CI: 0.623, 0.745), respectively, in external validation set 1 and 0.610 (95% CI: 0.449, 0.771) and 0.678 (95% CI: 0.512, 0.844), respectively, in external validation set 2.

The time-dependent discrimination measures for death are presented in Table S5. The time-dependent sensitivity was 77.3% for 1 year and 70.7% for 2 years in external validation set 1 and 87.9% for 1 year and 87.6% for 2 years in external validation set 2. Sensitivity represents the ability of the survival model to distinguish CIT group 1 (the lower-risk group) from the CIT groups 2–4 (the higher-risk groups).

Discussion

By evaluating patient data from a prospective registry, we developed a real-world survival model to stratify patients into four distinct risk groups according to gross total resection (GTR) of noncontrast-enhanced tumor (NET), age, and O^6-methylguanine-DNA methyltransferase promoter methylation status and validated this model in multinational external cohorts. GTR-NET was shown to be an independent predictor of overall survival (OS) and enabled patients to be stratified into lower- and higher-risk groups, with statistically significant differences in OS. The time-dependent sensitivity was consistent in both external sets, indicating that GTR-NET had good discrimination ability, because the lower-risk group had better survival. Our study highlights the importance of radiologic assessment of GTR-NET in preoperative and postoperative imaging, particularly because isocitrate dehydrogenase wild-type glioblastomas are increasingly recognized as noncontrast-enhanced infiltrative tumors under the WHO 2021 Classification of Tumors of the Central Nervous System guidelines.

GTR was found to be associated with increased OS, and many large retrospective cohort studies (6,7,24–28) have also demonstrated increased survival with increased EOR in patients with newly diagnosed glioblastoma. However, these studies were

conducted before the WHO 2021 classification scheme, which included high-grade gliomas with CETs without IDH testing. Similarly, in our study, patients who underwent GTR-NET had statistically significantly longer OS than those who did not (median OS, 32.6 vs 16.9 months, 30.4 vs 16.5 months, and 28.8 vs 15.8 months in the training set and external validation sets 1 and 2, respectively). Our study is meaningful because we included patients with IDH wild-type glioblastoma who exhibited extensive NETs, and among such patients, we found that GTR-NET was an independent prognostic marker of OS (HR, 0.30; $P <$ .001). Furthermore, we developed a CIT-based survival model to stratify patients into four distinct risk groups according to GTR-NET, age, and *MGMT* promoter methylation status. This survival model successfully stratified patients in external validation sets 1 and 2 into four distinct risk groups ($P <$ .001 and .04, respectively) with moderate performance (C-index, 0.65 and 0.63, respectively). The strength of our study is that the GTR status was assessed from a prospective registry of all those undergoing standard concurrent chemotherapy and radiation therapy, and the other variables matched, allowing assessment of the relevance of GTR on survival in an objective manner.

An important finding of our study is that in the CIT survival model, GTR-NET stands out as the primary determinant for patient risk categorization, underscoring the clinical significance of supramaximal resection. Considering that surgery is the sole prognostic factor actively pursued by clinicians, we recommend achieving maximum or complete resection of NET if possible. Although GTR-NET increases the likelihood of survival, damage to specific areas can reduce patients' quality of life. In such instances, the neurologic risk from potentially bordering functional cerebral areas needs to be weighed against the survival benefit of GTR-NET. Functionally guided resection, including preoperative diffusion tensor imaging scans to estimate white matter fiber tract location and awake craniotomy with cortical and subcortical stimulation, should help surgeons in achieving supramaximal resection while preserving critical functions.

A detailed discussion of our definition of GTR-NET related to supramaximal resection by the RANO group, management of CIT groups 2–4, and CIT survival model performance in external validation set 2 is available in Appendix S1.

Our study had limitations. First, the training set was derived from a prospective glioma registry, potentially including patients with better performance scores than a purely retrospective analysis. The comparability between registry data and other data (eg, randomized controlled trials) was acceptable according to previous literature (29). However, a strength of the registry is the objective measurement of patient outcomes. Additionally, the CIT survival model demonstrated moderate performance and calibration using external datasets from retrospective analyses, supporting the validity of our model. Second, we qualitatively assessed the EOR of NET, rather than strictly adhering to the definition from the RANO group (9), in which supramaximal resection is defined as 5 cm^3 or less residual NET. However, for the sampled cases, we conducted quantitative analysis of tumor volume using automated segmentation, making efforts to ensure that our qualitative assessment aligned well with the RANO group's quantitative definition. Finally, we did not assess the postoperative adverse effects potentially associated with supramaximal resection. Further investigations into these effects could provide a more comprehensive understanding of the implications of supramaximal resection in patients with IDH wild-type glioblastoma.

In conclusion, in patients with isocitrate dehydrogenase wild-type glioblastoma, gross total resection (GTR)–noncontrast-enhanced tumor (NET) is an independent prognostic factor for longer overall survival, regardless of age and O^6-methylguanine-DNA methyltransferase promoter methylation status. The GTR-NET–based survival model showed robustness in multinational validation. Our study provides evidence that radiologic assessment of the GTR of NET by preoperative and postoperative imaging is an important prognostic marker of glioblastoma.

Deputy Editor: Sven Haller
Scientific Editor: Shannyn Wolfe (AJE)

Author affiliations:

[1] Department of Radiology and Research Institute of Radiology, University of Ulsan College of Medicine, Asan Medical Center, 43 Olympic-ro 88, Songpa-Gu, Seoul 05505, Korea

[2] Department of Radiology, Oregon Health and Science University, Portland, Ore

[3] Department of Statistics and Epidemiology, University of Ulsan College of Medicine, Asan Medical Center, Seoul, Korea

[4] Department of Neurosurgery, University of Ulsan College of Medicine, Asan Medical Center, Seoul, Korea

[5] Department of Radiology and Research Institute of Radiological Science and Center for Clinical Imaging Data Science, Yonsei University College of Medicine, Seoul, South Korea

[6] Department of Radiology, Faculty of Medicine Siriraj Hospital, Mahidol University, Bangkok, Thailand

[7] Advanced Imaging Research Center, Oregon Health and Science University, Portland, Ore

[8] Knight Cancer Institute, Oregon Health and Science University, Portland, Ore

[9] Department of Statistics and Data Science, Korea National Open University, Seoul, Korea

Received May 12, 2024; revision requested June 12; revision received February 7, 2025; accepted February 14.

Address correspondence to: J.E.P. (email: jieunp@gmail.com).

Funding: This study was supported by the National Research Foundation of Korea by the Korean government (MSIP) (RS-2023-00208227, RS-2023-00305153). R.F.B. was supported by the National Institutes of Health National Cancer Institute (1R01CA288577, 1R21NS135452-01, K08CA237809, L30CA220897) and Jonathan D. and Mark C. Lewis Foundation.

Author contributions: Guarantors of integrity of entire study, **D.W., J.E.P., S.B., S.W.S., M.H.L., H.S.K.**; study concepts/study design or data acquisition or data analysis/interpretation, all authors; manuscript drafting or manuscript revision for important intellectual content, all authors; approval of final version of submitted manuscript, all authors; agrees to ensure any questions related to the work are appropriately resolved, all authors; literature research, **H.H.M., D.W., J.E.P., C.K.H., R.F.B., H.S.K.**; clinical studies, **H.H.M., D.W., J.E.P., Y.H.K., S.W.S., C.K.H., J.H.K., M.H.L., Y.W.P., S.S.A., J.A.P., R.F.B., H.S.K.**; experimental studies, **H.H.M., J.E.P., C.K.H., J.A.P., R.F.B.**; statistical analysis, **H.H.M., J.E.P., S.Y.P., S.B., C.K.H.**; and manuscript editing, **H.H.M., J.E.P., C.K.H., S.S.A., J.A.P., R.F.B., H.S.K.**

Data sharing: Data generated or analyzed during the study are available from the corresponding author by request.

Disclosures of conflicts of interest: **H.H.M.** No relevant relationships. **D.W.** No relevant relationships. **J.E.P.** No relevant relationships. **S.Y.P.** No relevant relationships. **S.B.** No relevant relationships. **Y.H.K.** No relevant relationships. **S.W.S.** No relevant relationships. **C.K.H.** No relevant relationships. **J.H.K.** No relevant relationships. **M.H.L.** No relevant relationships. **Y.W.P.** No relevant relationships. **S.S.A.** No relevant relationships. **J.M.P.** No relevant relationships. **R.F.B.** No relevant relationships. **H.S.K.** No relevant relationships.

References

1. Louis DN, Perry A, Wesseling P, et al. The 2021 WHO Classification of Tumors of the Central Nervous System: a summary. Neuro-oncol 2021;23(8):1231–1251.
2. Lacroix M, Abi-Said D, Fourney DR, et al. A multivariate analysis of 416 patients with glioblastoma multiforme: prognosis, extent of resection, and survival. J Neurosurg 2001;95(2):190–198.
3. Lao Y, Yu V, Pham A, et al. Quantitative Characterization of Tumor Proximity to Stem Cell Niches: Implications on Recurrence and Survival in GBM Patients. Int J Radiat Oncol Biol Phys 2021;110(4):1180–1188.
4. Lim DA, Cha S, Mayo MC, et al. Relationship of glioblastoma multiforme to neural stem cell regions predicts invasive and multifocal tumor phenotype. Neuro-oncol 2007;9(4):424–429.
5. Marko NF, Weil RJ, Schroeder JL, Lang FF, Suki D, Sawaya RE. Extent of resection of glioblastoma revisited: personalized survival modeling facilitates more accurate survival prediction and supports a maximum-safe-resection approach to surgery. J Clin Oncol 2014;32(8):774–782.
6. Cunha M, Esmeraldo ACS, Henriques LAW, Santos M Jr, Medeiros RTR, Botelho RV. Elderly patients with glioblastoma: the impact of surgical resection extent on survival. Rev Assoc Med Bras (1992) 2019;65(7):937–945.
7. Revilla-Pacheco F, Rodríguez-Salgado P, Barrera-Ramírez M, et al. Extent of resection and survival in patients with glioblastoma multiforme: Systematic review and meta-analysis. Medicine (Baltimore) 2021;100(25):e26432.
8. Dimou J, Beland B, Kelly J. Supramaximal resection: A systematic review of its safety, efficacy and feasibility in glioblastoma. J Clin Neurosci 2020;72:328–334.
9. Karschnia P, Young JS, Dono A, et al. Prognostic validation of a new classification system for extent of resection in glioblastoma: A report of the RANO resect group. Neuro-oncol 2023;25(5):940–954.
10. Lamborn KR, Chang SM, Prados MD. Prognostic factors for survival of patients with glioblastoma: recursive partitioning analysis. Neuro-oncol 2004;6(3):227–235.
11. Hertler C, Felsberg J, Gramatzki D, et al. Long-term survival with IDH wild-type glioblastoma: first results from the ETERNITY Brain Tumor Funders' Collaborative Consortium (EORTC 1419). Eur J Cancer 2023;189:112913.
12. Melhem JM, Detsky J, Lim-Fat MJ, Perry JR. Updates in IDH-wildtype glioblastoma. Neurotherapeutics 2022;19(6):1705–1723.
13. Stupp R, Mason WP, van den Bent MJ, et al; National Cancer Institute of Canada Clinical Trials Group. Radiotherapy plus concomitant and adjuvant temozolomide for glioblastoma. N Engl J Med 2005;352(10):987–996.
14. Wen PY, Chang SM, Van den Bent MJ, Vogelbaum MA, Macdonald DR, Lee EQ. Response assessment in neuro-oncology clinical trials. J Clin Oncol 2017;35(21):2439–2449.
15. Pope WB, Sayre J, Perlina A, Villablanca JP, Mischel PS, Cloughesy TF. MR imaging correlates of survival in patients with high-grade gliomas. AJNR Am J Neuroradiol 2005;26(10):2466–2474.
16. Lasocki A, Gaillard F, Tacey M, Drummond K, Stuckey S. Incidence and prognostic significance of non-enhancing cortical signal abnormality in glioblastoma. J Med Imaging Radiat Oncol 2016;60(1):66–73.
17. Lasocki A, Gaillard F. Non-contrast-enhancing tumor: a new frontier in glioblastoma research. AJNR Am J Neuroradiol 2019;40(5):758–765.
18. Moon HH, Park JE, Kim YH, Kim JH, Kim HS. Contrast enhancing pattern on pre-treatment MRI predicts response to anti-angiogenic treatment in recurrent glioblastoma: comparison of bevacizumab and temozolomide treatment. J Neurooncol 2022;157(3):405–415.
19. Karschnia P, Smits M, Reifenberger G, et al; Expert Rater Panel. A framework for standardised tissue sampling and processing during resection of diffuse intracranial glioma: joint recommendations from four RANO groups. Lancet Oncol 2023;24(11):e438–e450.
20. Tibshirani R. The lasso method for variable selection in the Cox model. Stat Med 1997;16(4):385–395.
21. Heagerty PJ, Zheng Y. Survival model predictive accuracy and ROC curves. Biometrics 2005;61(1):92–105.
22. Royston P, Moons KG, Altman DG, Vergouwe Y. Prognosis and prognostic research: Developing a prognostic model. BMJ 2009;338(mar31 1):b604.
23. Peduzzi P, Concato J, Feinstein AR, Holford TR. Importance of events per independent variable in proportional hazards regression analysis. II. Accuracy and precision of regression estimates. J Clin Epidemiol 1995;48(12):1503–1510.
24. Li YM, Suki D, Hess K, Sawaya R. The influence of maximum safe resection of glioblastoma on survival in 1229 patients: Can we do better than gross-total resection? J Neurosurg 2016;124(4):977–988.
25. Albert FK, Forsting M, Sartor K, Adams HP, Kunze S. Early postoperative magnetic resonance imaging after resection of malignant glioma: objective evaluation of residual tumor and its influence on regrowth and prognosis. Neurosurgery 1994;34(1):45–60; discussion 60–61.
26. Della Pepa GM, Ius T, La Rocca G, et al. 5-Aminolevulinic Acid and Contrast-Enhanced Ultrasound: The Combination of the Two Techniques to Optimize the Extent of Resection in Glioblastoma Surgery. Neurosurgery 2020;86(6):E529–E540.
27. Kim YJ, Lee DJ, Park CK, Kim IA. Optimal extent of resection for glioblastoma according to site, extension, and size: a population-based study in the temozolomide era. Neurosurg Rev 2019;42(4):937–950.
28. Molinaro AM, Hervey-Jumper S, Morshed RA, et al. Association of Maximal Extent of Resection of Contrast-Enhanced and Non-Contrast-Enhanced Tumor With Survival Within Molecular Subgroups of Patients With Newly Diagnosed Glioblastoma. JAMA Oncol 2020;6(4):495–503.
29. Levine MN, Julian JA. Registries that show efficacy: good, but not good enough. American Society of Clinical Oncology, 2008; 5316–5319.